AIP | Applied Physics Letters

# Enhanced separation of magnetic and diamagnetic particles in a dilute ferrofluid

Litao Liang, Cheng Zhang, and Xiangchun Xuan

Citation: Appl. Phys. Lett. **102**, 234101 (2013); doi: 10.1063/1.4810874
View online: http://dx.doi.org/10.1063/1.4810874
View Table of Contents: http://apl.aip.org/resource/1/APPLAB/v102/i23
Published by the American Institute of Physics.

# Enhanced separation of magnetic and diamagnetic particles in a dilute ferrofluid

Litao Liang,[1] Cheng Zhang,[2] and Xiangchun Xuan[1,a)]
[1]*Department of Mechanical Engineering, Clemson University, Clemson, South Carolina 29634-0921, USA*
[2]*Department of Mechanical Engineering, Georgia Southern University, Statesboro, Georgia 30460, USA*

(Received 10 May 2013; accepted 29 May 2013; published online 10 June 2013)

Traditional magnetic field-induced particle separations take place in water-based diamagnetic solutions, where magnetic particles are captured while diamagnetic particles flow through without being affected by the magnetic field. We demonstrate that replacing the diamagnetic aqueous medium with a dilute ferrofluid can significantly increase the throughput of magnetic and diamagnetic particle separation. This enhancement is attributed to the simultaneous positive and negative magnetophoresis of magnetic and diamagnetic particles, respectively, in a ferrofluid. The particle transport behaviors in both ferrofluid- and water-based separations are predicted using an analytical model. © *2013 AIP Publishing LLC*. [http://dx.doi.org/10.1063/1.4810874]

Separating target particles from a heterogeneous mixture is an important step in many chemical and biomedical applications. Magnetic field-induced particle separation[1–6] has a number of advantages over other methods (e.g., electric,[7,8] acoustic,[9,10] optical,[11,12] and hydrodynamic[13,14]) such as simplicity and low-cost.[15–19] Traditional magnetic field-induced particle separations, for example, magnetic-activated cell sorting (MACS),[20] take place in water-based diamagnetic solutions.[21–26] They rely on a full capture of magnetic particles inside a conduit while diamagnetic particles flow through it without being affected by an external magnetic field. This approach works well if the magnetic source is all around the conduit, which is, however, often not the case for lab-on-a-chip systems,[1–6,21–26] thereby limiting the particle throughput. We demonstrate herein that replacing the diamagnetic aqueous medium with a dilute ferrofluid can significantly increase the particle throughput of magnetic and diamagnetic particle separation in planar microchannels. This is verified through both experimental comparison and theoretical modeling. It is noted that similar ideas of re-suspending magnetic and diamagnetic particles into a magnetic solution have been recently reported to implement a simultaneous trapping of both types of particles in a paramagnetic solution[27] and a self-assembly of colloidal superstructures in a ferrofluid.[28,29]

Fig. 1 shows a picture of the microfluidic device used in our experiment. It was fabricated with polydimethylsiloxane (PDMS) using the standard soft lithography method as detailed elsewhere.[30] The T-shaped microchannel consists of one 400 $\mu$m-wide main-branch and two 200 $\mu$m-wide side-branches with a uniform depth of 40 $\mu$m. One neodymium-iron-boron (NdFeB) permanent magnet (B221, K&J Magnetics, Inc.) was embedded into the PDMS slab with the magnetization direction normal to the main-branch. It was placed 500 $\mu$m away from the main-branch and 3 mm from the side-branch (both are edge-to-edge distances). To demonstrate and compare the separations, 2.85 $\mu$m-diameter magnetic particles (Bangs Laboratories, Inc.) and 10 $\mu$m-diameter diamagnetic polystyrene particles (Duke Scientific Corp.) were mixed and re-suspended in two types of mediums: pure de-ionized (DI) water and 0.1× EMG 408 ferrofluid (Ferrotec Corp.), both to a final concentration of $10^6$–$10^7$ particles/ml. The particle suspension was driven through the microchannel by an infusion syringe pump (New Era Pump Systems, Inc.). The two outlet reservoirs were intentionally made large in order to reduce the effects of fluid buildup. Particle motion was visualized and recorded using an inverted microscope (Nikon Eclipse TE2000U, Nikon Instruments, Lewisville, TX) equipped with a CCD camera (Nikon DS-Qi1Mc). The obtained images were processed using the Nikon imaging software (NIS-Elements AR 2.30).

When a particle mixture in a ferrofluid flows through the main-branch of the T-microchannel (see Fig. 1), the suspended particles undergo a magnetophoretic motion, $\mathbf{U}_m$, due to the non-uniform magnetic field produced by the nearby permanent magnet[31–33]

$$\mathbf{U}_m = \frac{2a^2\mu_0[(\mathbf{M}_p - \mathbf{M}_f)\cdot\nabla]\mathbf{H}}{9\eta f_w}, \tag{1}$$

where $a$ is the particle radius, $\mu_0$ the free space permeability, $\mathbf{M}_p$ and $\mathbf{M}_f$ the magnetizations of the particle and the suspending ferrofluid, respectively, $\mathbf{H}$ the magnetic field at the particle center, $\eta$ the fluid viscosity, and $f_w$ the correction factor that accounts for the wall retardation effects on particle velocity.[30,34–37] With consideration of the self-demagnetization effect, the particle magnetization, $\mathbf{M}_p$, is given by[38–40]

$$\mathbf{M}_p = \frac{\chi_p}{1+\frac{1}{3}\chi_p}\mathbf{H}, \tag{2}$$

where $\chi_p$ is the particle magnetic susceptibility. The ferrofluid magnetization, $\mathbf{M}_f$, is collinear with the magnetic field, $\mathbf{H}$, and its magnitude is given by[41]

$$\frac{M_f}{\phi M_d} = \coth(\alpha) - \frac{1}{\alpha}, \tag{3}$$

a)Author to whom correspondence should be addressed. Electronic mail: xcxuan@clemson.edu. Fax: 864-656-7299.

 

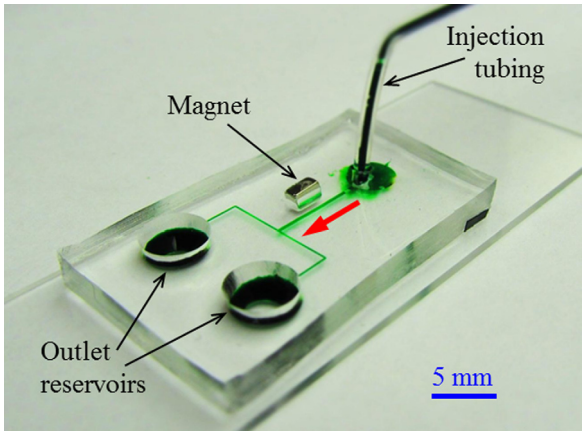


FIG. 1. Picture of the microfluidic device (the microchannel is filled with green food dye for clarity) used in experiment. The block arrow indicates the flow direction.

$$\alpha = \frac{\pi \mu_0 M_d H d^3}{6 k_B T}, \tag{4}$$

where $\phi$ is the volume fraction of magnetic nanoparticles in the ferrofluid, $M_d$ the saturation moment of the magnetic nanoparticles with an average diameter of $d$, $H$ the magnetic field magnitude, $k_B$ the Boltzmann constant, and $T$ the ferrofluid temperature.

Specifically, magnetic particles experience *positive* magnetophoresis in a dilute ferrofluid, i.e., $\mathbf{U}_m > 0$ due to $\mathbf{M}_p > \mathbf{M}_f$, and are pulled towards the magnet. On the contrary, diamagnetic particles experience *negative* magnetophoresis in a ferrofluid, i.e., $\mathbf{U}_m < 0$ due to $\mathbf{M}_p < \mathbf{M}_f$, and are pushed away from the high magnetic field region. Thus, as schematically shown in Fig. 2(a), the uniform particle mixture entering into the main-branch of the T-microchannel can be automatically divided into two distinct streams after passing through the magnet region. The sorted magnetic and diamagnetic particles will then each flow through one side-branch of the T-microchannel due to the even split of the ferrofluid flow at the T-junction, followed by a continuous collection at the corresponding outlet reservoir (see Fig. 1). This ferrofluid-based particle separation is superior to the traditional magnetic separation in a diamagnetic solution because magnetic particles must be completely trapped in the latter as schematically show in Fig. 2(b). Hence, the flow speed and, in turn, the particle throughput can be enhanced by the use of a ferrofluid, which will be demonstrated below through both experiment and modeling.

The trajectories of magnetic and diamagnetic particles during the separation process were simulated using a three-dimensional analytical model we developed earlier.[30] They were computed in MATLAB® by integrating the particle velocity, which was a vector addition of the suspending fluid velocity, $\mathbf{U}_f$, and the particle magnetophoretic velocity, $\mathbf{U}_m$, over time. The gravity and inertial effects on particle velocity were not considered.[30,34–39] The fluid flow was assumed to be fully developed in the main-branch, where the entrance and end (i.e., at the T-unction) effects were both assumed negligible under the experimental conditions. As such, $\mathbf{U}_f$ was referred to the well-known analytical formula for fluid velocity in a straight rectangular channel at a given flow

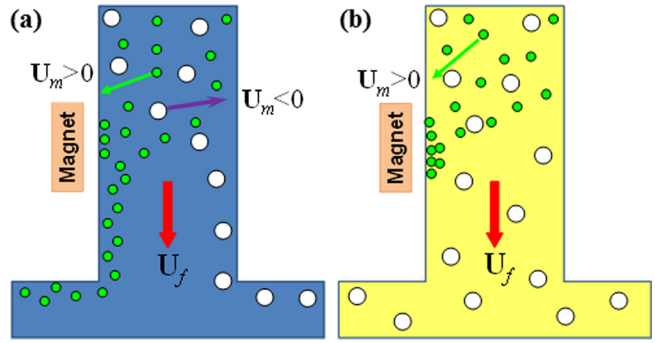


FIG. 2. Schematics illustrating and comparing the separation mechanisms of magnetic and diamagnetic particles suspended in 0.1× EMG 408 ferrofluid (a) and DI water (b), respectively. Note that $\mathbf{U}_m > 0$ and $\mathbf{U}_m < 0$ indicate the *positive* and *negative* magnetophoresis experienced by the magnetic and diamagnetic particles, respectively. The block arrow in each schematic indicates the direction of the suspending fluid.

rate.[42] The particle magnetophoretic velocity was calculated from Eq. (1), where the magnetic field was computed from Furlani's analytical model,[43] and the wall correction factor, $f_w$, was referred to Happel and Brenner.[44] The volume susceptibility of magnetic particles, $\chi_p = 0.024$, was extracted from the magnetization curve provided by the manufacturer for the range of magnetic field used in our experiment ($\sim 10^5$ A/m). The susceptibility of diamagnetic particles was set to zero. The magnetization of ferrofluid was calculated from Eq. (3) and that of water was neglected. Other parameters are referred to our earlier paper.[30]

Fig. 3 demonstrates the microfluidic separation of 2.85 $\mu$m magnetic particles and 10 $\mu$m diamagnetic particles in 0.1× EMG 408 ferrofluid (a) through a T-microchannel and also compares it against the magnetic separation of similar particles in DI water (b). The ferrofluid-based separation was achieved at a volume flow rate of 240 $\mu$l/h, equivalent to an average flow speed of about 4 mm/s. In contrast, the maximum flow rate at which magnetic particles can be fully captured by the magnet and thus be completely separated from the streaming diamagnetic particles is only 150 $\mu$l/h in water-based separation. This represents a 60% increase in particle throughput by the use of a diluted ferrofluid as the particle suspending medium. To illustrate and distinguish these two separation processes, a series of observation windows were used along with the flow in the main-branch of the T-microchannel, labeled as I-IV in Fig. 3. The relative positions of these four windows with respect to the magnet are schematically shown in the figure; specifically, window I is 3 mm ahead of the magnet; window II is after the front edge the magnet; window III is at the rear edge of the magnet; window IV is at the T-junction. The theoretically predicted trajectories of magnetic (red lines) and diamagnetic (green lines) particles in each of the observation windows are displayed besides the experimental images for both separations in Fig. 3.

In window I where the magnetic field is weak, magnetic and diamagnetic particles both follow the fluid streamlines and are uniformly mixed. No noticeable difference is experimentally observed for particle motions in between the ferrofluid- (presented in Fig. 3(a) as streak images which were obtained by superimposing a sequence of snapshot images) and water-based (presented in Fig. 3(b) as snapshot images)

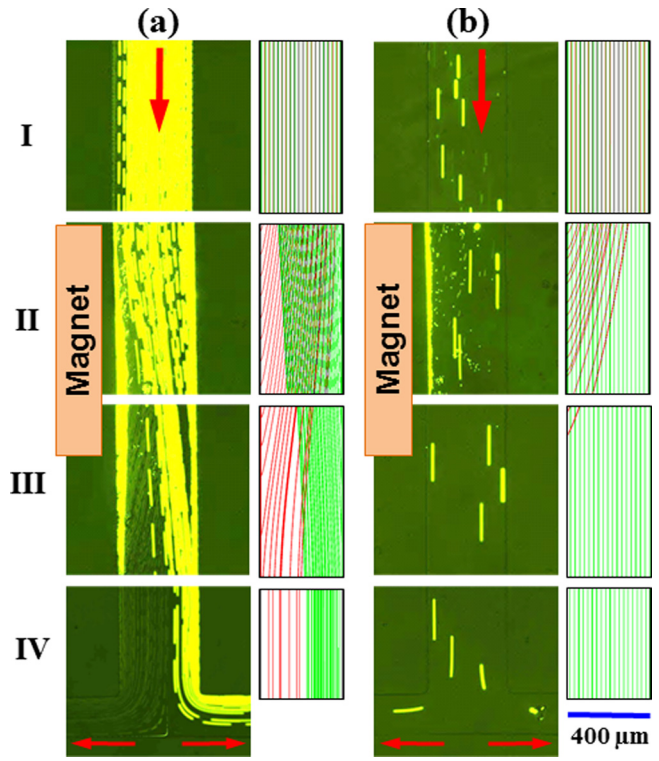


FIG. 3. Demonstration and comparison of the magnetic separation of 2.85 $\mu$m magnetic particles and 10 $\mu$m diamagnetic particles suspended in: (a) 0.1× EMG 408 ferrofluid at a volume flow rate of 240 $\mu$l/h (streak images); (b) DI water at 150 $\mu$l/h (snapshot images). The results are illustrated in four observation windows I–IV whose relative positions to the magnet are indicated by the schematic (not drawn to scale). The theoretically predicted trajectories of the two types of particles (red for magnetic and green for diamagnetic) in the main-branch of the T-microchannel are presented besides the experimental images for both cases. The block arrows indicate the flow direction.

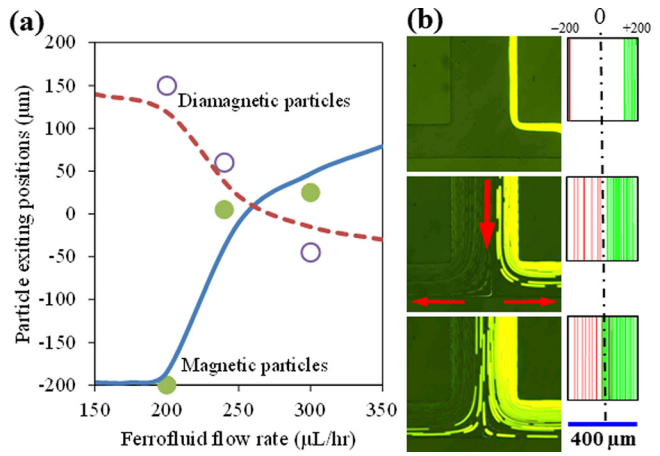


FIG. 4. Ferrofluid flow rate effects on the magnetic separation of 2.85 $\mu$m magnetic particles and 10 $\mu$m diamagnetic particles suspended in 0.1× EMG 408 ferrofluid: (a) compares the experimental (filled and hollow circles for magnetic and diamagnetic particles, respectively) and theoretical (solid and dashed lines for magnetic and diamagnetic particles, respectively) data for the particle positions [the closest relative to the channel centerline as highlighted by the dash-dotted line in (b)] exiting from the main-branch of T-microchannel; (b) shows the experimentally obtained streak images (left column) and theoretically predicted trajectories (right column, red and green lines for magnetic and diamagnetic particles, respectively) at the junction of the T-microchannel under the ferrofluid flow rate of 200 $\mu$l/h (top row), 240 $\mu$l/h (middle row), and 300 $\mu$l/h (bottom row), respectively.

separations. This is also confirmed by the theoretical modeling. When particles travel through the magnet region in windows II and III, however, apparent lateral deflections take place for both magnetic and diamagnetic particles suspended in the ferrofluid. Moreover, these two transverse motions are opposite to each other due to the induced positive and negative magnetophoresis, leading to a continuously increasing separation of the two types of particles. In contrast, only magnetic particles are attracted towards the magnet and captured in the water-based separation while diamagnetic particles still move straight through the channel without being affected by the magnet. These distinct particle deflection behaviors in the two separation processes are all reasonably predicted by the theoretical model. As particles approach the T-junction of the microchannel in window IV, a clear gap is formed between the two types of particles in ferrofluid-based separation. Following the even split of the ferrofluid flow, the magnetic and diamagnetic particles are continuously sorted into the left and right side-branches of the T-microchannel as seen from Fig. 3(a). In contrast, no magnetic particles escape from the magnet in water-based separation, and diamagnetic particles flow into the two side-branches at an equal rate as seen from the snapshot image in Fig. 3(b).

The effects of ferrofluid flow rate on the magnetic and diamagnetic particle separation are illustrated in Fig. 4(a), where the experimentally measured (symbols) and theoretically predicted (lines) particle exiting positions (the closest relative to the channel centerline) from the main-branch are compared. The experimental and theoretical data are obtained from the corresponding particle images at the T-junction in Fig. 4(b). As expected at a smaller flow rate than 240 $\mu$l/h (see the middle row of Figs. 4(b) and 3), both magnetic and diamagnetic particles attain a greater lateral deflection thereby facilitating their separation at the T-junction. This is clearly viewed from the particle streak images and trajectories at 200 $\mu$l/h in Fig. 4(b) (top row). Interestingly, we observed in our experiment that 2.85 $\mu$m magnetic particles can get fully trapped by the magnet, which is, however, not predicted by the theoretical model. This deviation is speculated to be due to the influence of the locally concentrated magnetic nanoparticles in the ferrofluid near the magnet, which is not taken into consideration in our model. When the ferrofluid flow rate gets larger than 240 $\mu$l/h, the magnetic and diamagnetic particle streams start overlapping at the T-junction with the decrease in their respective lateral deflections. This causes an incomplete separation as demonstrated by the particle images at 300 $\mu$l/h in Fig. 4(b) (bottom row). Overall one can see from Fig. 4(a) that the theoretical model is able to predict the exiting positions of magnetic and diamagnetic particles with a reasonable agreement. We are currently developing a numerical model to account for the ferrofluid concentration effects on particle transport.

In summary, we have demonstrated a microfluidic separation of 2.85 $\mu$m-diameter magnetic and 10 $\mu$m-diameter diamagnetic particles in 0.1× EMG 408 ferrofluid through a T-microchannel. Such a ferrofluid-based magnetic separation can offer a significantly higher particle throughput than the corresponding water-based separation due to an induced negative magnetophoresis of diamagnetic particles in the

ferrofluid. We have also developed a 3D analytical model to simulate the transport and separation of magnetic and diamagnetic particles in both suspending fluids, which agree reasonably with the experimental observations. Future work will be on the bio-applications of the proposed ferrofluid-based particle separation.

This work was supported by NSF under Grant No. CBET-1150670 (Xuan).

[1]N. Pamme, Lab Chip **6**, 24–38 (2006).
[2]C. Liu, T. Stakenborg, S. Peeters, and L. Lagae, J. Appl. Phys. **105**, 102014 (2009).
[3]M. A. M. Gijs, F. Lacharme, and U. Lehmann, Chem. Rev. **110**, 1518–1563 (2010).
[4]M. Suwa and H. Watarai, Anal. Chim. Acta **690**, 137–147 (2011).
[5]M. Zborowski and J. J. Chalmers, Anal. Chem. **83**, 8050–8056 (2011).
[6]Q. Ramadan and M. A. M. Gijs, Microfluid. Nanofluid. **13**, 529–542 (2012).
[7]R. Pethig, Biomicrofluidics **4**, 022811 (2010).
[8]J. Regtmeier, R. Eichhorn, M. Viefhues, L. Ogunovic, and D. Anselmetti, Electrophoresis **32**, 2253–2273 (2011).
[9]T. Laurell, F. Peterson, and A. Nilsson, Chem. Soc. Rev. **36**, 492–506 (2007).
[10]S. Lin, X. Mao, and T. Huang, Lab Chip **12**, 2766–2770 (2012).
[11]S. H. Cho, J. M. Godin, C. Chen, W. Qiao, H. Lee, and Y. Lo, Biomicrofluidics **4**, 043001 (2010).
[12]A. A. Kayani, K. Khoshmanesh, S. A. Ward, A. Mitchell, and K. Kalantar-zadeh, Biomicrofluidics **6**, 031501 (2012).
[13]H. Tsutsui and C. M. Ho, Mech. Res. Commun. **36**, 92–103 (2009).
[14]D. Di Carlo, Lab Chip **9**, 3038–3046 (2009).
[15]N. Pamme, Lab Chip **7**, 1644–1659 (2007).
[16]A. Lenshof and T. Laurell, Chem. Soc. Rev. **39**, 1203–1217 (2010).
[17]A. A. S. Bhagat, H. Bow, H. Hou, S. Tan, J. Han, and C. Lim, Med. Biol. Eng. Comput. **48**, 999–1014 (2010).
[18]D. R. Gossett, W. M. Weaver, A. J. Mach, S. C. Hur, H. T. Tse, W. Lee, H. Amini, and D. Di Carlo, Anal. Bioanal. Chem. **397**, 3249–3267 (2010).
[19]A. Karimi, S. Yazai, and A. M. Ardekani, "Hydrodynamic mechanisms of cell and particle trapping in microfluidics," Biomicrofluidics **7**, 021501 (2013).
[20]B. Schmitz, A. Radbruch, T. Kümmel, C. Wickenhauser, H. Korb, M. L. Hansmann, J. Thiele, and R. Fischer, Eur. J. Haematol. **52**, 267–275 (1994).
[21]D. W. Inglis, R. Riehn, R. H. Austin, and J. C. Sturm, Appl. Phys. Lett. **85**, 5093–5095 (2004).
[22]D. W. Inglis, R. Riehn, J. C. Sturm, and R. H. Austin, J. Appl. Phys. **99**, 08K101 (2006).
[23]E. Mirowski, J. Moreland, A. Zhang, S. E. Russek, and M. J. Donahue, Appl. Phys. Lett. **86**, 243901 (2005).
[24]K. Hoshino, Y. Y. Huang, N. Lane, M. Huebschman, J. W. Uhr, E. P. Frenkel, and X. Zhang, Lab Chip **11**, 3449–3457 (2011).
[25]J. H. Kang, S. Krause, H. Tobin, A. Mammoto, M. Kanapathipillai, and D. E. Ingber, Lab Chip **12**, 2175–2181 (2012).
[26]N. T. Nguyen, Microfluid. Nanofluid. **12**, 1–16 (2012).
[27]M. D. Tarn, S. A. Peyman, and N. Pamme, RSC Adv. **3**, 7209–7214 (2013).
[28]R. M. Erb, H. S. Son, B. Samanta, V. M. Rotello, and B. B. Yellen, Nature (London) **457**, 999–1002 (2009).
[29]K. H. Li and B. B. Yellen, Appl. Phys. Lett. **97**, 083105 (2010).
[30]L. Liang, J. Zhu, and X. Xuan, Biomicrofluidics **5**, 034110 (2011).
[31]G. Friedman and B. Yellen, Curr. Opin. Colloid Interface Sci. **10**, 158–166 (2005).
[32]R. M. Erb and B. Yellen, *Nanoscale Magnetic Materials and Applications*, edited by J. P. Liu (Springer, 2009), pp. 563–590.
[33]L. Liang and X. Xuan, Biomicrofluidics **6**, 044106 (2012).
[34]T. Zhu, R. Cheng, and L. Mao, Microfluid. Nanofluid. **11**, 695–701 (2011).
[35]T. Zhu, D. J. Lichlyter, M. A. Haidekker, and L. Mao, Microfluid. Nanofluid. **10**, 1233–1245 (2011).
[36]J. Zhu, L. Liang, and X. Xuan, Microfluid. Nanofluid. **12**, 65–73 (2012).
[37]T. Zhu, R. Cheng, S. A. Lee, E. Rajaraman, M. A. Eiteman, T. D. Querec, E. R. Unger, and L. Mao, Microfluid. Nanofluid. **13**, 645–654 (2012).
[38]A. Sinha, R. Ganguly, A. K. De, and I. K. Puri, Phys. Fluid. **19**, 117102 (2007).
[39]S. S. H. Tsai, I. M. Griffiths, and H. A. Stone, Lab Chip **11**, 2577–2582 (2011).
[40]E. P. Furlani and X. Xue, Microfluid. Nanofluid. **13**, 589–602 (2012).
[41]R. E. Rosensweig, "Magnetic fluids," Annu. Rev. Fluid. Mech. **19**, 437–463 (1987).
[42]F. M. White, *Viscous Fluid Flow* (McGraw-Hill, 1991).
[43]E. P. Furlani, *Permanent Magnet and Electromechanical Devices: Materials, Analysis, and Applications* (Academic Press, 2001).
[44]J. Happel and H. Brenner, *Low Reynolds Number Hydrodynamics* (Springer, 1973).